TECHNISCHE MECHANIK, Band 23, Heft 1, (2003), 70-80
Manuskripteingang: 22. November 2002

Modelling of Plastic Anisotropy and Plastic Volume Change

W. Ripplinger, M. Schultz, M. Hein, H. Ismar

An anisotropic material law for metallic materials is presented which is able to describe plastic volume changes in the elastic-plastic transition area. The modelling includes a mixed isotropic-kinematic hardening rule. The strategy of evolution is used to fit the material law to yield loci of X5CrNi18.10. The additional extension of the model by anisotropic hardening permits the description of the deformation anisotropy. Finally, the plane compression of a thick cylinder is used to show the effect of the material law used. Therefore the outer radius is equally reduced and the deformation behaviour of the inner radius is observed.

1 Introduction

Nowadays many metal forming processes can be simulated with the aid of computers. Such a simulation always works with models that allow only an idealized description of reality. Thus, it is important that the modelling should represent the real behaviour of the material used as closely as possible. For the application, the flow potential of v.Mises (1913) is that which is nowadays mostly used. It assumes that the material properties are independent of the examined direction (isotropy). Thus, the real behaviour is represented too imprecisely. Many metallic materials show a more or less distinct mechanical anisotropy. To predict the forming behaviour of these materials an extended anisotropic material law is required.

Furthermore, examinations of X5CrNi18.10 have shown a plastic volume change at the starting point of plastic deformation in uniaxial tensile tests (Ismar, 1987). Also the flow potential of v.Mises cannot express this behaviour. In the current study an anisotropic flow potential is presented which can describe the dependence of the direction of deformation as well as the plastic volume change at the elastic-plastic area of transition in a more natural-like manner.

2 Fundamentals of Constitutive Modelling

To describe the plastic yielding at one point of a metallic material, the continuum mechanics uses the flow potential $\mathrm{F}(\sigma_{ij})$, which has the value of a scalar. The flow potential depicts the transition from elastic to elastic-plastic behaviour with the help of the flow condition:

$$\mathrm{F}(\sigma_{ij}) - \mathrm{f}(\sigma_f) = \text{const.} \tag{1}$$

In equation (1) the multiaxial state of stress is compared to a function that depends on the uniaxial yield stress σ_f. The flow condition can be graphically interpreted as the yield surface in the principal stress space. The vectors of stress ending within this surface mean an elastic behaviour of the associated point of the material. A state of stress which is exactly on the surface causes plastic deformation. If the centre of the subsequent yield surface is moved by ζ_{ij} compared to the initial surface (kinematic hardening), the reduced stress

$$s_{ij} = \sigma_{ij} - \zeta_{ij} \tag{2}$$

will be used in equation (1) instead of the stress coordinates. Most of the metals can be described by a flow potential in the form of

$$\mathrm{F} = \mathrm{F}(\mathrm{I}_1^{\mathbf{s}}, \mathrm{I}_2^{\mathbf{s}'}) = \text{const.} \tag{3}$$

Here $\mathrm{I}_1^{\mathbf{s}} = s_{ii}$ is the first invariant of the tensor $\mathbf{s}$ and $\mathrm{I}_2^{\mathbf{s}'} = \frac{1}{2}(s_{ij}\, s_{ij})$ the second invariant of the deviatoric reduced stress $\mathbf{s}'$ with $s'_{ij} = s_{ij} - \frac{1}{3} s_{kk}\, \delta_{ij}$.

The plastic strain increment $d\varepsilon_{ij}^{p}$ is linked to the stresses by the potential flow rule:

$$d\varepsilon_{ij}^{p} = d\lambda \cdot \frac{\partial \mathrm{F}}{\partial \sigma_{ij}} \tag{4}$$

The nonnegative scalar proportionality constant $d\lambda$ depends on the deformation history for potentials that have a form as in equation (3).
The most used description of the plastic behaviour of metals is the isotropic flow potential of v.Mises (1913). Combined with a potential level (isotropic hardening) that depends on the equivalent plastic strain ε_{v}^{p}, the yield criterion is obtained by considering the kinematic hardening:

$$\mathrm{F} = \sqrt{3\,\mathrm{I}_2^{s'}} - \sigma_f\,(\varepsilon_v^p) = 0 \tag{5}$$

The increment of equivalent plastic strain $d\varepsilon_{v}^{p}$ is determined by comparing the differentials of the dissipated plastic work of the uniaxial and the multiaxial loading cases:

$$\sigma_{ij}\, d\varepsilon_{ij}^{p} = \sigma_f \cdot d\varepsilon_{v}^{p} \tag{6}$$

In the principal stress space equation (5) defines an indefinitely long circular cylinder whose generating lines are parallel to the space diagonal $(\sigma_{\mathrm{I}} = \sigma_{\mathrm{II}} = \sigma_{\mathrm{III}})$. With this, the v.Mises potential assumes plastic volume constancy during plastic deformation.

An improved modelling of plastic compressible materials is made possible by the isotropic transition flow potential. This comprises the hydrostatic pressure which is described by the first invariant of the stress tensor (Mahrenholtz, Ismar 1979):

$$\mathrm{F} = \sqrt{\frac{\alpha\,\mathrm{I}_1^{s^2} + \mathrm{I}_2^{s'}}{\alpha + \frac{1}{3}}} - \sigma_f = 0 \tag{7}$$

The scalar internal function α is always positive (convexity of the yield surface) and depends only on the equivalent plastic strain ε_{v}^{p}. This potential results in the principal stress space in an ellipsoid of revolution whose semi-major axis is identical to the space diagonal. α declines to zero even under small equivalent plastic strains ε_{v}^{p}. Consequently, the yield surface geometry progresses with increasing plastic deformation from the ellipsoid of revolution into the v.Mises cylindrical yield surface.

A well known anisotropic flow potential was developed by Hill (1950). It refers to the orthogonal anisotropy. On the basis of the potential of v.Mises (equation (5)), Hill also uses a quadratic structure. In the principal stress space it has the form

$$\mathrm{F} = a_1 \cdot (s_{\mathrm{II}} - s_{\mathrm{III}})^2 + a_2 \cdot (s_{\mathrm{I}} - s_{\mathrm{III}})^2 + a_3 \cdot (s_{\mathrm{I}} - s_{\mathrm{II}})^2 - \bar{\sigma}^2 \tag{8}$$

with the constants a_1, a_2, a_3 describing the anisotropy, the reduced principal stresses $s_{\mathrm{I}}, s_{\mathrm{II}}, s_{\mathrm{III}}$ and a stress of reference $\bar{\sigma}$.

As described in (Hill, 1979) Hill replaces the quadratic exponents by the exponents *m*, thus making a better fit of the potential equation (8) to some experimental data. Furthermore he expands the potential by adding the deviator stresses of the principal directions. Each of these is weighted with its own coefficient of anisotropy a_4, a_5, a_6:

$$\begin{aligned}\mathrm{F} = {} & a_1 \cdot (s_{\mathrm{II}} - s_{\mathrm{III}})^m + a_2 \cdot (s_{\mathrm{I}} - s_{\mathrm{III}})^m + a_3 \cdot (s_{\mathrm{I}} - s_{\mathrm{II}})^m + a_4 \cdot (2s_{\mathrm{I}} - s_{\mathrm{II}} - s_{\mathrm{III}})^m + \\ & + a_5 \cdot (2s_{\mathrm{II}} - s_{\mathrm{I}} - s_{\mathrm{III}})^m + a_6 \cdot (2s_{\mathrm{III}} - s_{\mathrm{I}} - s_{\mathrm{II}})^m - \bar{\sigma}^m\end{aligned} \tag{9}$$

To avoid modulus in equation (9) there will be a restriction to whole-numbered and even-numbered values of *m*.

For an anisotropic flow potential, Barlat (1991) avails himself of the isotropic potential of Hosford (1972). He replaces its isotropic deviator stresses by the appropriate anisotropic deviator stresses:

$$\mathrm{F} = (s_{\mathrm{II}}^* - s_{\mathrm{III}}^*)^m + (s_{\mathrm{I}}^* - s_{\mathrm{III}}^*)^m + (s_{\mathrm{I}}^* - s_{\mathrm{II}}^*)^m - 2\bar{\sigma}^m \tag{10}$$

with

$$
\begin{aligned}
s_{\mathrm{I}}^{*} &= \tfrac{1}{3}\left((c_3 + c_2)\cdot s_{\mathrm{I}} - c_3 \cdot s_{\mathrm{II}} - c_2 \cdot s_{\mathrm{III}}\right) \\
s_{\mathrm{II}}^{*} &= \tfrac{1}{3}\left(-c_3 \cdot s_{\mathrm{I}} + (c_1 + c_3)\cdot s_{\mathrm{II}} - c_1 \cdot s_{\mathrm{III}}\right) \\
s_{\mathrm{III}}^{*} &= \tfrac{1}{3}\left(-c_2 \cdot s_{\mathrm{I}} - c_1 \cdot s_{\mathrm{II}} + (c_1 + c_2)\cdot s_{\mathrm{III}}\right) \\
c_1, c_2, c_3 &: \text{ constants to describe the anisotropy}
\end{aligned}
\tag{11}
$$

Karafillis and Boyce present in (Karafillis, 1993) an extension of the flow potential equation (10). They supplement the potential by a second term via a weighting factor *c*:

$$
\begin{aligned}
\mathrm{F} = (1-c)\cdot\left[(s_{\mathrm{II}}^{*} - s_{\mathrm{III}}^{*})^{m} + (s_{\mathrm{I}}^{*} - s_{\mathrm{III}}^{*})^{m} + (s_{\mathrm{I}}^{*} - s_{\mathrm{II}}^{*})^{m}\right] + \\
+ c\cdot\frac{3^{m}}{2^{m-1}+1}\cdot\left(s_{\mathrm{I}}^{*\,m} + s_{\mathrm{II}}^{*\,m} + s_{\mathrm{III}}^{*\,m}\right) - 2\bar{\sigma}^{m}
\end{aligned}
\tag{12}
$$

To describe the plastic anisotropy in the present study, another extension of equation (10), as was developed in (Barlat, 1995) will be used. This potential law includes the plastic volume constancy and is described in principal stresses by

$$
\mathrm{F} = a_1\cdot(s_{\mathrm{II}}^{*} - s_{\mathrm{III}}^{*})^{m} + a_2\cdot(s_{\mathrm{I}}^{*} - s_{\mathrm{III}}^{*})^{m} + a_3\cdot(s_{\mathrm{I}}^{*} - s_{\mathrm{II}}^{*})^{m} - 2\bar{\sigma}^{m} \tag{13}
$$

with the anisotropic deviator stresses of equation (11). With the six anisotropic coefficients (a_1, a_2, a_3, c_1, c_2, c_3) and the exponent *m*, this potential can easily be fitted to experimental data. In (Barlat, 1995) equation (13) is presented as a six-component yield function. The shear stresses are weighted by their own anisotropic factor. The general stress state equation (13) can be expressed as

$$
\mathrm{F} = a_1\cdot\mathrm{f}_1^{m} + a_2\cdot\mathrm{f}_2^{m} + a_3\cdot\mathrm{f}_3^{m} + a_4\cdot s_{12}^{m} + a_5\cdot s_{23}^{m} + a_6\cdot s_{13}^{m} - \bar{\sigma}^{m} \tag{14}
$$

with

$$
\begin{aligned}
\mathrm{f}_1 &= s_{\mathrm{I}}^{*} - s_{\mathrm{II}}^{*} = \tfrac{1}{3}\left((c_2 + 2c_3)\cdot s_{11} - (c_1 + 2c_3)\cdot s_{22} + (c_1 - c_2)\cdot s_{33}\right) \\
\mathrm{f}_2 &= s_{\mathrm{II}}^{*} - s_{\mathrm{III}}^{*} = \tfrac{1}{3}\left((c_2 - c_3)\cdot s_{11} + (2c_1 + c_3)\cdot s_{22} - (2c_1 + c_2)\cdot s_{33}\right) \\
\mathrm{f}_3 &= s_{\mathrm{III}}^{*} - s_{\mathrm{I}}^{*} = \tfrac{1}{3}\left(-(2c_2 + c_3)\cdot s_{11} + (c_3 - c_1)\cdot s_{22} + (c_1 + 2c_2)\cdot s_{33}\right)
\end{aligned}
\tag{15}
$$

To describe the plastic volume change at the beginning of the plastic deformation as well as the anisotropic behaviour of the material, the first invariant of the stress tensor will be added to equation (14) analogously to equation (7). The stress of reference $\bar{\sigma}$ is identical to the yield stress in the direction of $\mathbf{e}_{\mathrm{II}}$. Thus the anisotropic transition flow potential is

$$
\mathrm{F} = \sqrt[m]{\frac{(\alpha'\cdot s_{ii})^{m} + a_1\cdot\mathrm{f}_1^{m} + a_2\cdot\mathrm{f}_2^{m} + a_3\cdot\mathrm{f}_3^{m} + a_4\cdot s_{12}^{m} + a_5\cdot s_{23}^{m} + a_6\cdot s_{31}^{m}}{\alpha'^{m} + \mathrm{f}_4(a_i, c_i)}} - \bar{\sigma} \tag{16}
$$

with the analogous scalar internal function α' (which is described in detail in section 4) and

$$
\mathrm{f}_4(a_i, c_i) = \frac{1}{3^{m}}\left(a_1\cdot(c_1 + 2c_3)^{m} + a_2\cdot(2c_1 + c_3)^{m} + a_3\cdot(c_3 - c_1)^{m}\right) \tag{17}
$$

For the anisotropic transition flow potential, the scalar proportionality constant $d\lambda$ introduced in equation (4) is identical to the increment of the equivalent plastic strain $d\varepsilon_v^{p}$. This can be deduced with the aid of equation (6).

The increment of the plastic volume strain, derived from equation (4), is

$$
\frac{dV}{V} = d\varepsilon_{ii}^{p} = 3\,d\varepsilon_v^{p}\cdot\frac{\alpha'^{m}}{\alpha'^{m} + \mathrm{f}_4(a_i, c_i)}\cdot\left(\frac{s_{ii}}{\sigma_v(s_{ij})}\right)^{m-1} \tag{18}
$$

with the following equivalent stress:

$$
\sigma_v(s_{ij}) = \sqrt[m]{\frac{(\alpha'\cdot s_{ii})^{m} + a_1\cdot\mathrm{f}_1^{m} + a_2\cdot\mathrm{f}_2^{m} + a_3\cdot\mathrm{f}_3^{m} + a_4\cdot s_{12}^{m} + a_5\cdot s_{23}^{m} + a_6\cdot s_{31}^{m}}{\alpha'^{m} + \mathrm{f}_4(a_i, c_i)}} \tag{19}
$$

3 Hardening

In addition to a suitable flow potential a capable hardening law is necessary for a lifelike modelling of the plastic material behaviour. There are various different types of hardening.

Isotropic hardening is characterized by a mere enlargement of the yield surface. In doing so, it maintains its shape, location and orientation in the stress space. With this type of hardening the stress of reference $\overline{\sigma}$ in the yield criterion is described by the equivalent plastic strain ε_v^p:

$$\sigma_v(\sigma_{ij}) - \overline{\sigma}(\varepsilon_v^p) = 0 \tag{20}$$

In this case the progression of $\overline{\sigma}$ is identical to that of the yield stress which can be described with (Hopperstad, 1998):

$$\sigma_f\ (\varepsilon_v^p) = \sigma_{f0} + \sum_{\mathrm{i}} q_i \cdot \left(1 - \mathrm{e}^{(-r_i \cdot \varepsilon_v^p)}\right) \tag{21}$$

The number of terms in equation (21) is arbitrary, but normally it is sufficient to use i = 2. The constants q_i and r_i describe the hardening of the material.

The geometry of the yield surface remains the same during the plastic deformation, if the kinematic hardening law is used. There is a straight movement of the yield surface. Then the yield criterion is

$$\sigma_v(s_{ij}) - \sigma_{f0} = 0 \tag{22}$$

with $\sigma_{f0} = \text{const.}$

A few theories exist concerning the direction of the movement of the surface. The approach by Ziegler (1959) is used in the current study. Accordingly the translation is in the direction of the reduced stress s_{ij}, which is the connection of the centre of the yield surface with the current point of stress.

The mixed isotropic-kinematic hardening rule takes both parts into account. Therefore, the positive mixed hardening parameter ξ is used to represent the ratio of isotropic hardening to the total hardening as a function of the actual equivalent plastic strain ε_v^p. Thus, the yield criterion has the form

$$\sigma_v\left(\sigma_{ij} - \zeta_{ij}(\varepsilon_v^p)\right) - \overline{\sigma}(\varepsilon_v^p) = 0 \tag{23}$$

with

$$\overline{\sigma}(\varepsilon_v^p) = \xi \cdot \sigma_f\ (\varepsilon_v^p) \tag{24}$$

and

$$d\zeta_{ij} = \left(\frac{\partial \sigma_f}{\partial \varepsilon_v^p} - \frac{\partial \overline{\sigma}}{\partial \varepsilon_v^p}\right) \cdot d\varepsilon_v^p \cdot \frac{s_{ij}}{\sigma_v} \tag{25}$$

The experimental study of the mixed hardening parameter shows a dependence of the equivalent plastic strain and can be represented by

$$\xi\left(\varepsilon_v^p\right) = 1 - \xi_1 \cdot \left(1 - \mathrm{e}^{-\xi_2 \cdot \varepsilon_v^p}\right) - \xi_3 \cdot \left(1 - \mathrm{e}^{-\xi_4 \cdot \varepsilon_v^p}\right) \tag{26}$$

4 Identification of the Parameters

The parameters of the material law are obtained for the corrosion resistant austenitic steel X5CrNi18.10 using experimental ascertained yield loci. The used thin-walled tubular specimens are annealed at 860°C for two hours (solution annealing) and then slowly cooled in the furnace. The Vickers hardness of this annealed steel is in the range of 161 HV20.

Similarly to the isotropic transition flow potential, the parameter α' declines to zero under small equivalent plastic strains (Figure 1). The curve can be approximated by

$$\alpha'\left(\varepsilon_v^p\right) = 0.7113 \cdot \mathrm{e}^{(-53000 \cdot \varepsilon_v^p)} \tag{27}$$

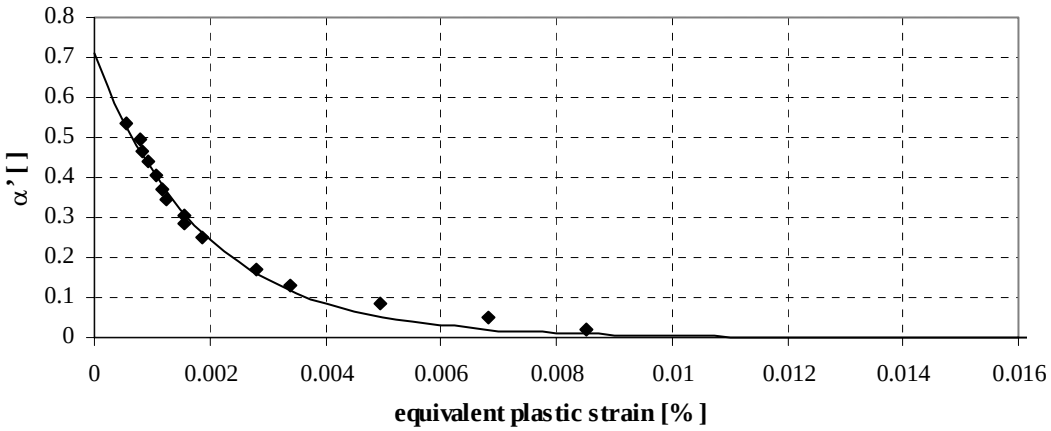

Figure 1: Scalar Internal Function α' (X5CrNi18.10)

The part of the flow potential responsible for the plastic volume strain, also disappears if $\alpha' = 0$. The closed yield surface then progresses into a cylindrical yield surface. During the subsequent plastic deformation the material shows plastic volume constancy.

After the unloading and a subsequent plastic deformation of the material, it can be seen that the value of α' is again greater than zero. But the value is less than that of the first deformation. In the elastic area, the yield surface again progresses to a closed convex surface. Figure 2 shows the scalar internal function α' during a periodically elastic-plastic swell loading.

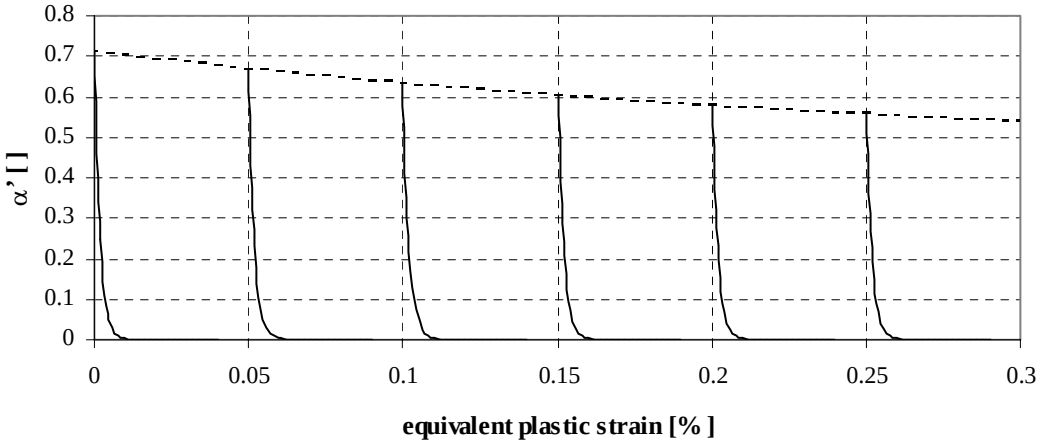

Figure 2: Scalar Internal Function during a Swell Loading (X5CrNi18.10)

To describe α' the current value of the equivalent plastic strain and the ε_{v0}^p existing at the unloading are required:

$$\alpha'\left(\varepsilon_v^p, \varepsilon_{v0}^p\right) = \alpha'_{st}\left(\varepsilon_{v0}^p\right) \cdot \mathrm{e}^{(-s \cdot \varepsilon_v^p)} \tag{28}$$

where s is the decay constant and $\alpha'_{st}\left(\varepsilon_{v0}^p\right)$ the launch value according to

$$\alpha'_{st}\left(\varepsilon_{v0}^p\right) = k_0 + k_1 \cdot \mathrm{e}^{(-k_2 \cdot \varepsilon_{v0}^p)} \tag{29}$$

Equation (29) shows that the launch values do not decline to zero, but there remains a plateau level k_0 at a sufficiently large plastic deformation. The nondimensional material parameters s and k_i are summarized in Table 1.

	s	k_0	k_1	k_2
X5CrNi18.10	53000	0.2663	0.445	350

Table 1: Parameters for Describing the Scalar Internal Function α'

With the aid of some stress-strain-curves the yield stress curve equation (21) is obtained. The unknown parameters q_1, q_2, r_1, r_2 (i = 2) are determined by means of an optimization method, the strategy of evolution (Table 2).

	σ_{f0} [N/mm²]	q_1 [N/mm²]	r_1 [ ]	q_2 [N/mm²]	r_2 [ ]
X5CrNi18.10	141.3	77.65	303.3	57.42	18291

Table 2: Parameters for Describing the Yield Stress Curve

In order to study the hardening of the material, the tube specimens were deformed with uniaxial tension or compression to a greater or lesser extent. After unloading, another uniaxial deformation causes an axial stress σ_{II} in the wall of the tube. An additional internal or external pressure generates a circumferential stress σ_I. Thus there is a biaxial state of stress in the wall of the tube. By this means, various points of the yield locus in the $\sigma_I - \sigma_{II}$ – plane of principal stress are obtained. Every point is the result of the average value of three experiments. The degrees of deformation used are 0% (S), 20% (T1, C1), 33% (T2, C2) and 55% (T3) above σ_{f0}.

For the determination of the mixed hardening parameter ξ, the experimental uniaxial yield stress of tension (σ_{fT}) and compression (σ_{fC}) is required for every degree of deformation (Figure 3).

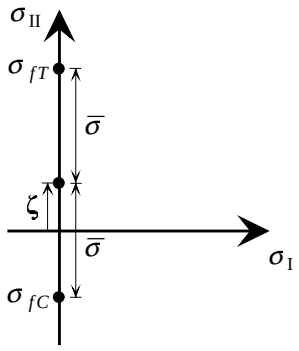

Figure 3: Yield Stress of Uniaxial Tension and Compression
with Preceding Tensile Deformation

The displacement of the centre point of the yield surface is in the direction of the external load. Consequently the centre point bisects the line between σ_{fT} and σ_{fC}. Thus, with the aid of these stresses, the absolute value of the vector of displacement ζ and the stress of reference $\bar{\sigma}$ can be obtained. The latter is identical to the distance between the centre point and one of the yield stresses.

$$\begin{aligned} \bar{\sigma} &= \frac{1}{2}(k_{fT} - k_{fC}) \\ |\zeta| &= \zeta_{II} = \frac{1}{2}(k_{fT} + k_{fC}) \end{aligned} \tag{30}$$

The mixed hardening parameter ξ of an undeformed specimen is (equation (24)):

$$\xi = \frac{\bar{\sigma}}{\sigma_f} \tag{31}$$

To obtain the appropriate equivalent plastic strain, equation (21) is required together with the corresponding value of σ_f. Again the unknown parameters ξ_i of equation (26) are determined via the strategy of evolution:

$$\xi\left(\varepsilon_v^p\right)=1-0.0945\cdot\left(1-\mathrm{e}^{-442.6\cdot\varepsilon_v^p}\right)-0.7045\cdot\left(1-\mathrm{e}^{-17760\cdot\varepsilon_v^p}\right) \tag{32}$$

Figure 4 shows the comparison of the experimental data and the appropriate yield loci obtained with the potential of v.Mises. It should be noted that the distance between the yield stress in the direction of the loading and that after reversal of the loading visibly shrinks as a function of the degree of deformation. This effect is designated as softening. Furthermore it seems that the yield stress in the direction of σ_I is nearly independent of the degree of deformation. In this way the diameter of the surface remains almost constant. The representation of the non-quadratic course which emerges noticeably from the experimental data is insufficient in this case of the isotropic material law.

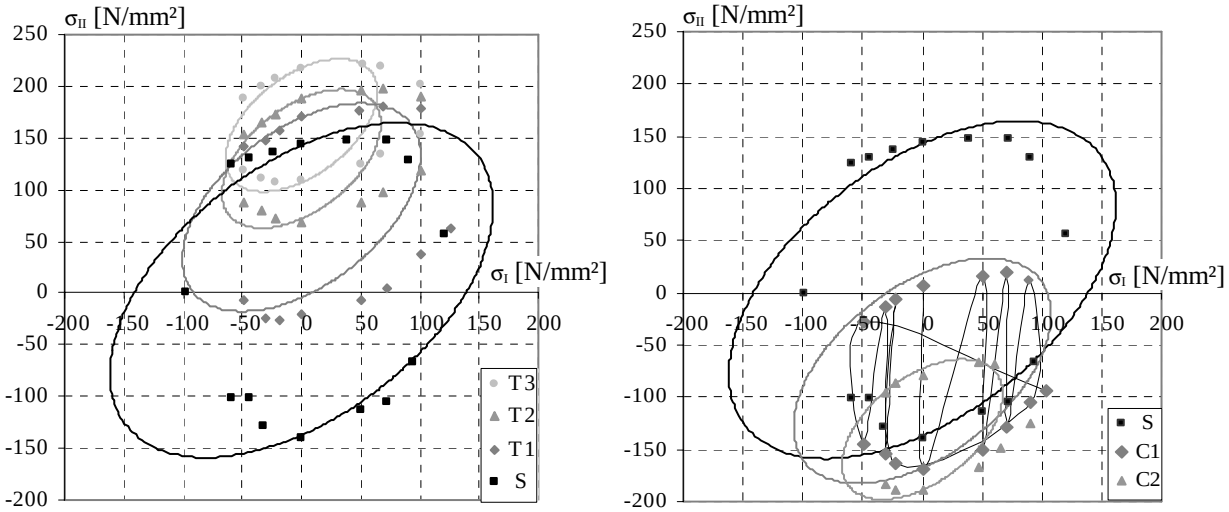

Figure 4: Comparison of Experimental Starting Points of Plastic Deformation and Yield Loci of the Isotropic Material Law of v.Mises

For the optimization of the parameters, the experimentally obtained starting points of plastic deformation have been weighted according to their standard deviation (scatter). Thereby it is guaranteed, that “reliable” measured values such as the uniaxial yield stress are on the yield locus. The optimization of the parameters for the anisotropic transition flow potential equation (16) is carried out for different exponents m (m = 2, 4, 6, 8, 10) via the strategy of evolution. The best set of parameters is attained for m = 8 and is shown in Table 3. As can be seen in Figure 5, this model is more suitable for predicting the experimental data, but is still not sufficient.

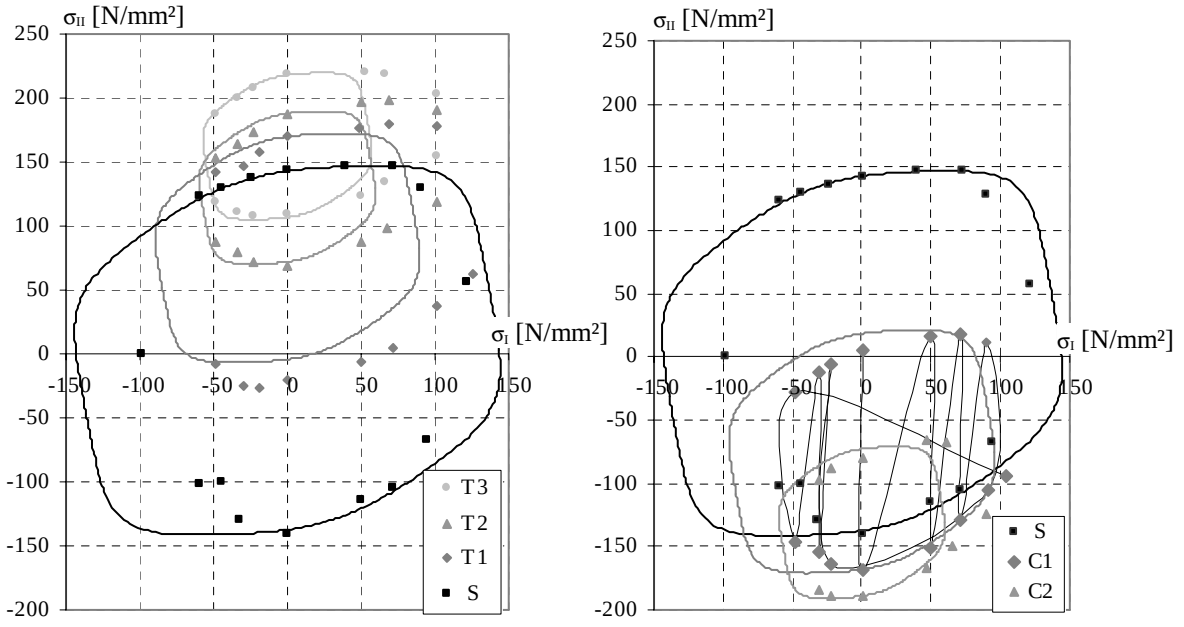

Figure 5: Comparison of Experimental Starting Points of Plastic Deformation and Yield Loci of the Anisotropic Transition Flow Potential

	m	a_1	a_2	a_3	a_4, a_5, a_6	c_1	c_2	c_3
X5CrNi18.10	8	0.2338	0.4102	5.2002	4356	2.1314	1.3372	1.4677

Table 3: Parameters for Describing the Plastic Anisotropy in Equation (16)

For an improved predictability a larger modification of the shape of the yield surface must be possible. This is not given with the isotropic-kinematic hardening. The shape of the surface is defined by the parameters of anisotropy. The examination of a possible change in the parameters shows a dependence of the appropriate equivalent plastic strain:

$$a_i(\varepsilon_v^p) = a_{i0} + a_{i1} \cdot \left(1 - \mathrm{e}^{-a_{i2} \cdot \varepsilon_v^p}\right)$$
$$c_i(\varepsilon_v^p) = c_{i0} + c_{i1} \cdot \left(1 - \mathrm{e}^{-c_{i2} \cdot \varepsilon_v^p}\right) \tag{33}$$

Thus the modification of the yield surface is greatest at the beginning of the deformation and declines with an increasing degree of deformation. By this means the anisotropic hardening can be described, which is also known as anisotropy of deformation (Lippmann, 1981). Consequently there are 18 values for the parameters of anisotropy and one exponent for an optimal fit of the material law to the experimental data. At m = 4 the renewed optimization of the parameters results in the values of Table 4.

X5CrNi18.10	a_{i0}, c_{i0}	a_{i1}, c_{i1}	a_{i2}, c_{i2}
a_1	0.0978	6.3410	1310
a_2	0.9852	-0.6572	7373
a_3	0.9363	-0.7923	4672
c_1	0.7925	1.5278	10365
c_2	1.2046	-0.2198	21277
c_3	1.2263	-1.1355	849.7

Table 4: Parameters for Describing the Plastic Anisotropy at m = 4

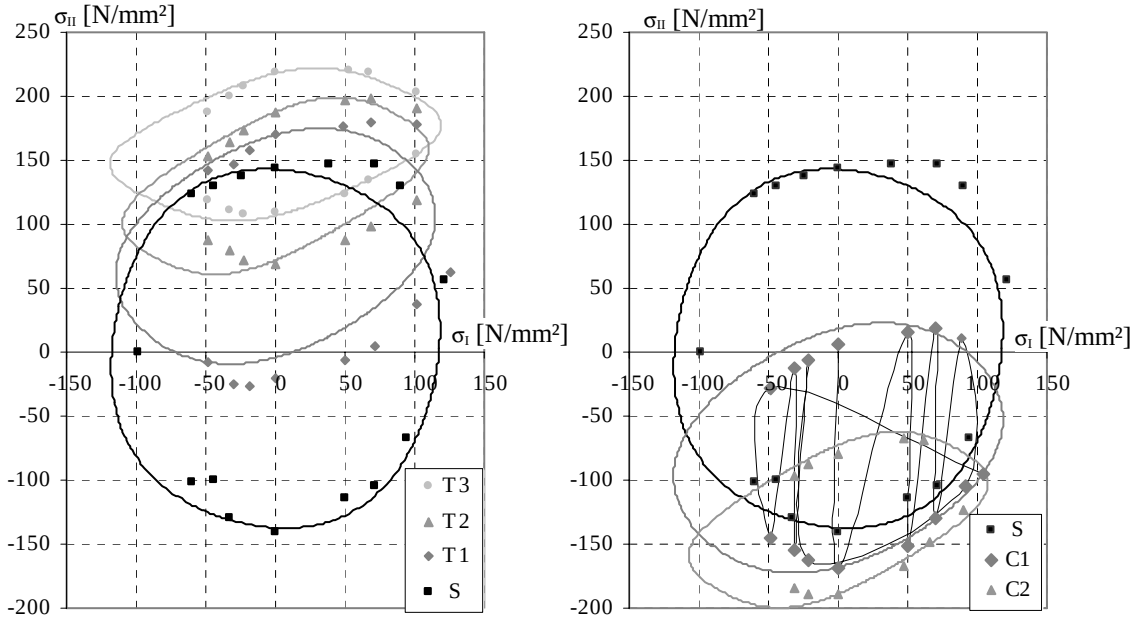

Figure 6: Comparison of Experimental Starting Points of Plastic Deformation and Yield Loci of the Anisotropic Transition Flow Potential with Anisotropic Hardening

With the enhancement of the model the experimental data are essentially more natural-like, as can be seen in Figure 6. The constancy of the diameter of the yield loci in the direction of σ_I is identifiable. This behaviour cannot be described by the purely isotropic-kinematic hardening law.

5 Plane Deformation of a Thick Cylinder

The following example of application serves as a demonstration of the difference between the simple isotropic transition flow potential and the more natural-like anisotropic potential. The simulation is about the plane deformation of a thick cylinder and the outer radius of the cylinder is reduced from 60 mm to 50 mm. The inner radius at the initial state amounts to 40 mm (Figure 7 left). The directions of the axis of anisotropy resulting from the experimental data are arranged in such a way that $\mathbf{e}_I$ lies in the horizontal and $\mathbf{e}_{II}$ in the vertical direction. Because of the symmetries, it is sufficient to discretise a quarter of the annulus. The boundary conditions resulting from the symmetry are shown on the right-hand side of Figure 7. The outer radius is moved stepwise in a radial direction towards the centre and the behaviour of the inner radius is observed. The cylinder maintains a constant thickness of 1 mm during the deformation (plane deformation). The elastic characteristics are expected to be isotropic.

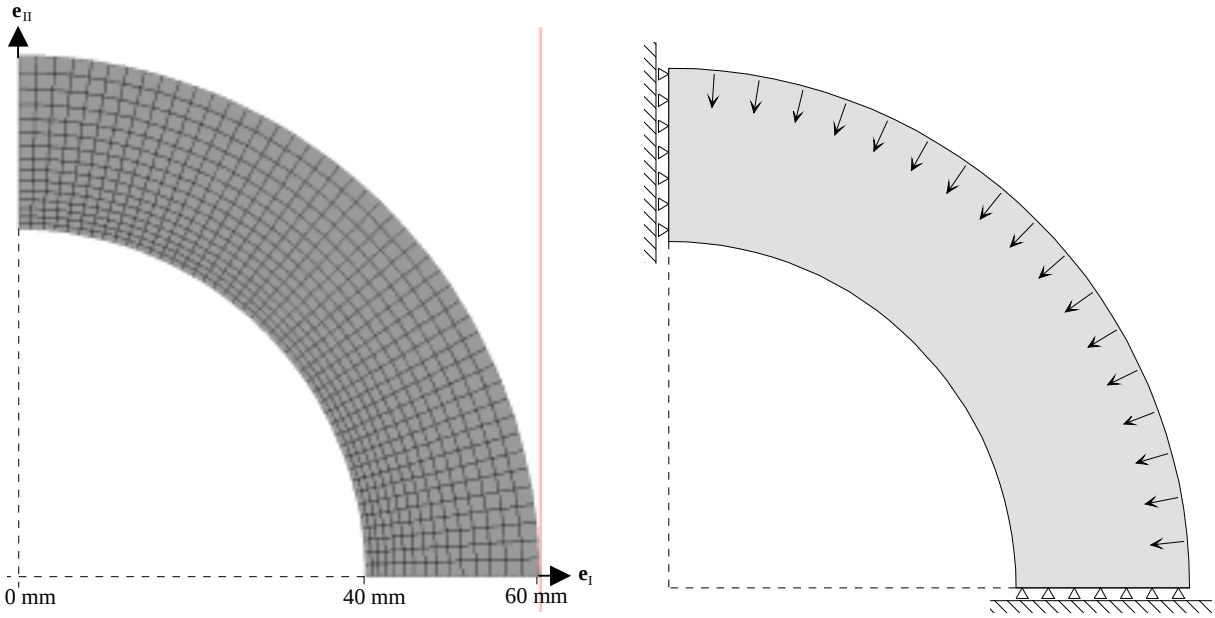

Figure 7: Discretisation and Boundary Conditions of the Quarter of the Cylinder

If the parameters of the isotropic transition flow potential are chosen, the inner radius must move equally towards the centre and the circular shape must be obtained. This expected behaviour of an isotropic material law is correctly reproduced by the simulation (Figure 8). To clarify the deformation, the initial state of the cylinder is also shown.

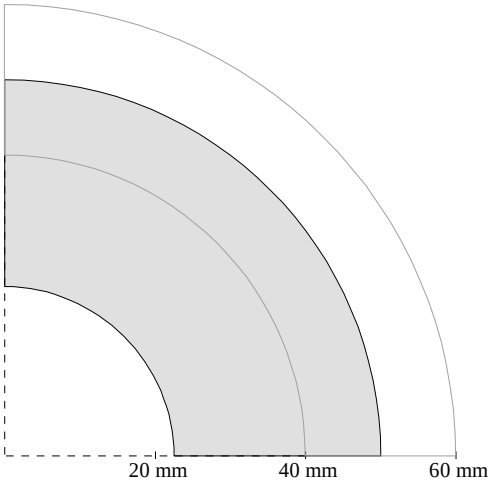

Figure 8: Shape of the Cylinder Calculated with the Isotropic Transition Flow Potential Equation (7)

The shape of the inner radius becomes non-circular if the anisotropic transition flow potential with constant and respectively variable parameters is used, as can be seen in Figure 9. At the range of $\varphi = 22.5°$ and 67.5° the inner radius bulges towards the centre. Both versions of the anisotropic material law result in a similar shape of the radius. The shape of the radii for the different sets of parameter is depicted in Figure 10. The direction of angle φ is demonstrated in Figure 9.

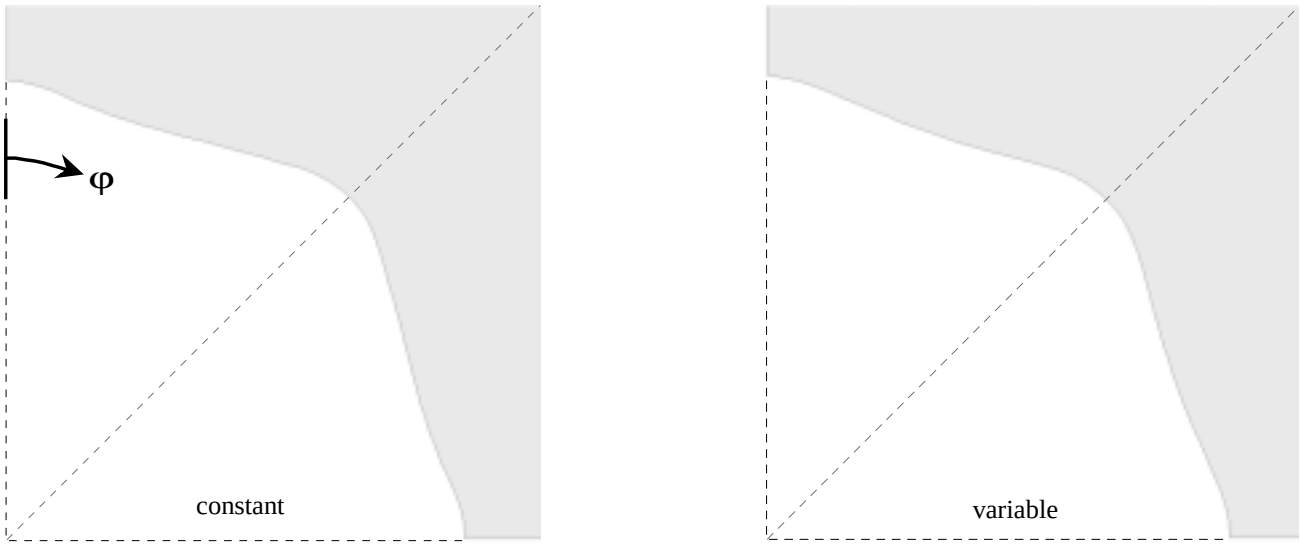

Figure 9: Shape of the Inner Radius Calculated with Constant and Variable Parameters of Anisotropy

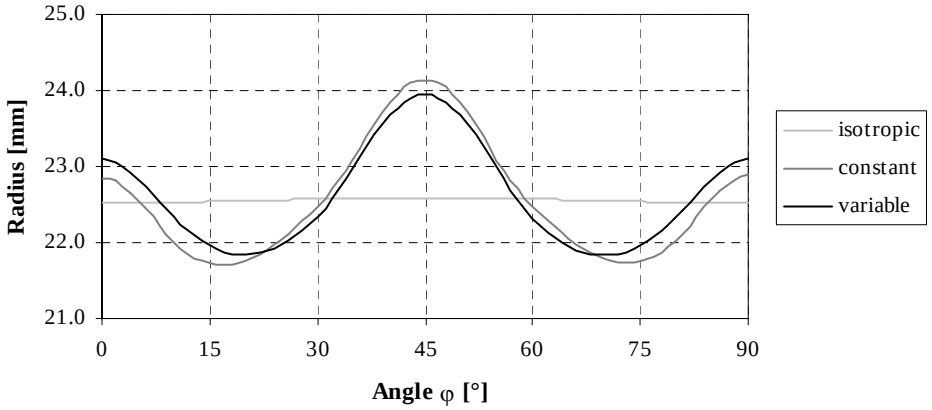

Figure 10: Comparison of the Shapes of the Inner Radius after Deformation

At $\varphi = 45°$ the radius has its maximum. The divergence of the circular shape is not negligible. At the narrowest location, the radius is 0.7 mm smaller than that of the simulation with the isotropic material law.

Figure 11 shows the comparison of the necessary deformation energy during deformation for the various material laws. Both sets of anisotropic parameters predict a higher deformation energy than in the isotropic case. One reason for this is the enormous deformation at $\varphi = 45°$. In spite of the similar shape of the inner radius, the use of the variable parameters is reasonable. Otherwise the prediction of the energy needed for the deformation process is too low.

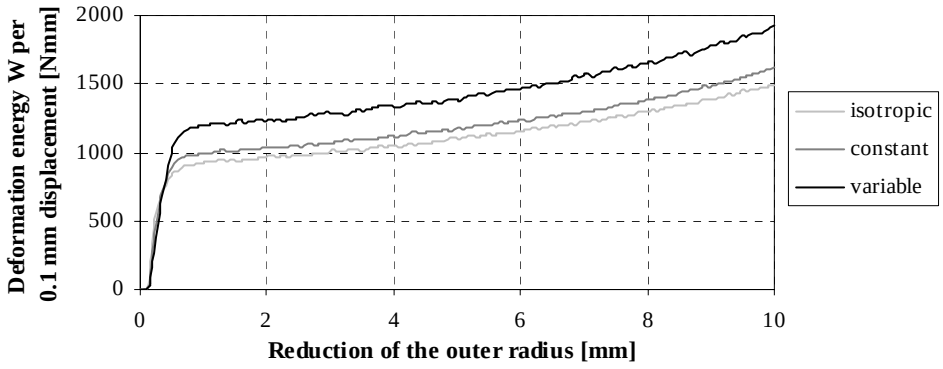

Figure 11: Deformation Energy per 0.1 mm Displacement of the Outer Radius

6 Summary

The experimental determination of yield loci of X5CrNi18.10 reveals a distinct anisotropic behaviour combined with softening during the deformation. Furthermore the material shows a plastic volume change in the transition area between elastic and elastic-plastic deformation. The anisotropy and the volume change can be described by a material law based on an anisotropic flow potential and including the first invariant of the stress tensor. With a mixed isotropic-kinematic hardening law it is possible to predict experimental data with a deformation history. If there is a change in the shape of the yield surface during forming, this can be modeled by a dependency of the parameters of anisotropy by the equivalent plastic strain. Also it is then possible to use this model for other materials with anisotropy and plastic volume change such as metal foams, or at the occurrence of phase transitions during the deformation.

References

Barlat, F.; Lege, D.J.; Brem, J.C.: A six-component yield function for anisotropic materials, Int. J. Plast., 7, (1991), 693-712.

Barlat, F.; Maeda, Y.; Yanagawa, M.: Yielding description of solution strengthened aluminium alloys, Proceedings of the Fourth International Conference on Computational Plasticity, Pineridge Press, Barcelona, (1995), 879-888.

Hill, R.: The mathematical theory of plasticity, Oxford University Press, New York, (1950).

Hill, R.: Theoretical plasticity of textured aggregates, Math. Proc. Camb. Phil. Soc., 85, (1979), 179-191.

Hopperstad, O.S.; Berstad, T.; Ilstad, H.: Effects of the yield criterion on local deformations in numerical simulation of profile forming, J. Mat. Proc. Tech., 80-81, (1998), 551-555.

Hosford, W.F.: A generalized isotropic yield criterion, J. Appl. Mech., 39, (1972), 607-609.

Ismar, H.; Schmitt, A.; Sutor, J.: Zur Beanspruchung metallischer Werkstoffe im Bereich der Elastizitätsgrenze, Forsch. Ing., 53, (1987), 162-168.

Karafillis, A.P.; Boyce, M.C.: A general anisotropic yield criterion using bounds and a transformation weighting tensor, J. Mech. Phys. Solids, 41, (1993), 1859-1886.

Lippmann, H.: Mechanik des plastischen Fließens, Springer-Verlag, Berlin/Heidelberg, (1981).

Mahrenholtz, O.; Ismar, H.: Ein Modell des elastisch-plastischen Übergangsverhaltens metallischer Werkstoffe, Abhandlung d. Braunschw. Wiss. Gesellschaft, 30, (1979), 138-144.

Mises, R.v.: Mechanik des festen Körpers im plastisch deformablen Zustand, Nachr. Königl. Ges. Wiss. Göttingen, math. Phys. Kl., (1913), 582-592.

Ziegler, H.: A modification of Prager's hardening rule; Quat. Appl. Math., 17, (1959), 55-65.

Address: Dr.-Ing. W. Ripplinger, Dr.-Ing. M. Schultz, Dipl.-Ing. M. Hein, Prof. Dr.-Ing. H. Ismar,
Lehrstuhl für Technische Mechanik, Universität des Saarlandes, Postfach 15 11 50, D-66041 Saarbrücken,
e-mail: w.ripplinger@mx.uni-saarland.de